IEEE Access
Multidisciplinary | Rapid Review | Open Access Journal

Received February 4, 2018, accepted March 13, 2018, date of publication March 28, 2018, date of current version April 23, 2018.

Digital Object Identifier 10.1109/ACCESS.2018.2820175

Two-Stage Non-Orthogonal Multiple Access Over Power Line Communication Channels

KHALED M. RABIE[1], (Member, IEEE), BAMIDELE ADEBISI[1], (Senior Member, IEEE), ANDREA M. TONELLO[2], (Senior Member, IEEE), SERHAN YARKAN[3], (Member, IEEE), AND MUHAMMAD IJAZ[1], (Member, IEEE)

[1]School of Electrical Engineering, Manchester Metropolitan University, Manchester M15 6BH, U.K.
[2]Institute of Networked and Embedded Systems, University of Klagenfurt, Klagenfurt 9020, Austria
[3]Center for Applied Research on Informatics Technologies, Istanbul Commerce University, 34840 Istanbul, Turkey

Corresponding author: Khaled M. Rabie (k.rabie@mmu.ac.uk)

This work was supported by the Innovate U.K. through the CityVerve: IoTs and Smart Cities Demonstrator Project under Grant 102561.

ABSTRACT Non-orthogonal multiple access (NOMA) has recently been proposed for dual-hop cooperative relaying power line communication (PLC) systems. Unlike conventional NOMA-PLC schemes which deploy NOMA only at the relay, this paper proposes to enhance the performance of such systems by implementing the principle of NOMA at both the source and relaying modems. The system performance is evaluated in terms of the average sum capacity for which analytical expressions are derived for both the improved and conventional NOMA-PLC systems. Throughout our analysis, the PLC channel is assumed narrow-band modeled with log-normal amplitude distribution and the total PLC noise consists of both background and impulsive noise. Monte Carlo simulations are provided to corroborate the accuracy of our theoretical analysis. The derived expressions are utilized to examine the impact of various system parameters on the average capacity performance; this includes: impulsive noise probability, network branching, power allocation coefficients, and transmit power. The optimization problem of the power allocation coefficients is also addressed for both NOMA-PLC systems under consideration. Results reveal that significant gains in the average capacity can be attained with the improved NOMA-PLC approach compared to the conventional system. In addition, the improved system is able to meet a given performance requirement with smaller transmit power offering more relaxed electromagnetic compatibility issues associated with PLCs. Finally, it is demonstrated that optimizing the power allocation coefficients at both the source and relay modems is crucial to maximize performance.

INDEX TERMS Average capacity, cooperative relaying, impulsive noise, log-normal fading, non-orthogonal multiple access (NOMA), power line communication (PLC).

I. INTRODUCTION

Power line communication (PLC) is a promising technology that is able to provide efficient, robust and cost-effective solutions to many home-networking and smart grid applications. Although it is true that power lines do not represent a favorable communication medium compared to the conventional ones such as wireless and fiber optics [1]–[3], advancement and development in signal processing and modulation techniques have made reliable and secure communications over power lines possible. An example of these techniques is multi-carrier modulation such as orthogonal frequency division multiplexing (OFDM) which is widely adopted by most standardization and industrial bodies [4], [5]. OFDM was shown to be more robust to many PLC channel impairments including frequency-selectivity and the non-Gaussian noise [6]–[8].

Cooperative relaying over power lines can reduce the effect of attenuation and losses making communication in this network more efficient and reliable. Numerous studies have analyzed various relaying protocols, including amplify-and-forward (AF) and decode-and-forward (DF), in the context of PLCs; see e.g., [9]–[12]. Relaying also allows using smaller transmit power at PLC modems which can considerably reduce electromagnetic emissions. All the work above, however, is based on orthogonal multiple access (OMA) in the sense that transmissions between PLC modems are accomplished through time division multiple access (TDMA); this however is spectral inefficient. To overcome this issue, non-orthogonal multiple access (NOMA), which allows simultaneous data transmission for different users (modems) at the same time and frequency with different power levels, was recently explored in PLC networks. More

specifically, Rabie *et al.* [13] analyzed the performance of a NOMA-based dual-hop DF cooperative relaying narrow-band PLC system. In this work, the source modem transmits two data symbols with different power allocation factors during the first phase; both the relay and destination receive the superposition coded signal during this phase. The destination decodes the signal with higher power while treating the other as noise. At the relay, the higher power signal is also decoded, first, and then canceled using successive interference cancellation (SIC) to obtain the second symbol. In the second phase, with the assumption that it is successfully decoded, the relay will forward the second symbol to the destination. Although this proposed system was shown to offer considerable performance enhancement in comparison to the orthogonal cooperative relaying PLC approach, the achievable performance gain is rather limited since the principle of NOMA is only implemented at one modem, i.e., the source; this approach will be referred to as the conventional NOMA-PLC system.

Unlike [13], in this study we implement NOMA at both the source and relay modems; i.e., a two-stage power allocation NOMA scheme will be deployed. More specifically, in contrast to [13], where the relay forwards only the secondly decoded symbol, in the current work, the relay forwards the two symbols with new power allocation coefficients. The other difference between the conventional and improved NOMA-PLC systems is that the destination modem does not decode the signal received from the source in the latter until it also receives the relayed version and then jointly decodes the two symbols with equal gain combining. This clearly overcomes the capacity limitation caused by decoding the symbol transmitted over the highly attenuated source-to-destination link in the conventional NOMA-PLC system. It should be noted that the general motivation for using NOMA in PLC systems is two-fold. First, NOMA allows to use reduced transmit power at PLC modems (as will be shown later) which can further relax the electromagnetic compatibility (EMC) problem associated with PLCs. Second, NOMA provides better fairness among users since it allows to transmit multiple signals simultaneously to different users (PLC modems) with each user occupying the entire bandwidth.

The contributions of this paper are as follows. An accurate analytical expression for the average capacity of the improved NOMA-PLC system is derived. For the sake of comparison, the capacity performance of the conventional NOMA-PLC is also investigated. These analytic derivations of capacity bring interesting new results both in the methodology and in the overall assessment of performance in PLC channels affected by log-normal attenuation and impulsive noise. Another contribution of this study resides in examining the impact of several system parameters on the capacity performance for the two systems under consideration. In addition, the optimization problem of the power allocation coefficients for the two NOMA-PLC systems is addressed. In all our investigations, Monte Carlo simulations are provided to verify the accuracy of the theoretical analysis. It is worthwhile mentioning that DF relaying is adopted in this work, and not AF, not only because the former can offer better performance but also because AF relaying over impulsive noise PLC channels does not always enhance performance as was recently found by Facina *et al.* [14]. Results show that the improved NOMA-PLC system can offer considerable gains in terms of average capacity relative to the conventional NOMA-PLC system reported in [13]. It is also demonstrated that as the probability occurrence of impulsive noise and the channel variance are increased, the performance of both systems considered will degrade. Furthermore, optimizing the power allocation coefficients at both the source and relay modems plays an important role to maximize the overall system capacity.

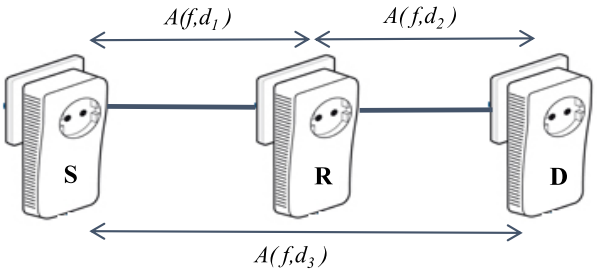

FIGURE 1. The considered system model consisting of three PLC modems: a source (S), a relay (R) and a destination (D).

The rest of this paper is organized as follows. Section II describes the system model for both the improved and conventional NOMA-PLC systems. Section III derives analytical expressions for the average capacity for the two systems under consideration. Results and discussions are presented in Section IV. Finally, Section V concludes the paper and outlines the main remarks.

The following notations are used in this paper. $f_X(\cdot)$, $F_X(\cdot)$ and $\bar{F}_X(\cdot)$ represent the probability density function (PDF), cumulative distribution function (CDF) and complementary CDF (CCDF), respectively. Also, $\min\{\cdot\}$ denotes the minimum argument and $\mathbb{E}\{\cdot\}$ is the statistical expectation operator. By $\Pr\{\cdot\}$, we refer to the probability function.

II. SYSTEM MODEL

Fig. 1 illustrates the system model under study which consists of three PLC modems: a source, a relay and a destination. A narrow-band PLC network is considered with a relay based on DF protocol operating in half-duplex mode. It is assumed that there exists a direct link between the end modems and that channel state information (CSI) is perfectly known at all receiving modems. The source-to-relay (sr), relay-to-destination (rd) and source-to-destination (sd) channel coefficients are complex valued with amplitudes denoted as $h_{\rm sr}$, $h_{\rm rd}$ and $h_{\rm sd}$, respectively, whereas $d_{\rm sr}$, $d_{\rm rd}$ and $d_{\rm sd}$ represent the corresponding distances. The amplitude of all the channel coefficients are assumed to follow log-normal distribution, [15]–[17], with a PDF

$$f(h_m) = \frac{1}{\sqrt{2\pi}\sigma_m h_m} \exp\left(-\frac{(\ln(h_m) - \mu_m)^2}{2\sigma_m^2}\right), \quad (1)$$

where $m \in \{\text{sr, rd, sd}\}$, μ_m and σ_m^2 represent respectively the mean and the standard deviation of $10\log_{10}(h_m)$. It is known that PLC channels suffer from frequency- and distance-dependent attenuation which will be represented in our analysis as $A_m(f, d_m)$ with f being the operating frequency and and d_m denotes the m-th distance [1], [18]–[20].

The communication is accomplished over two consecutive time slots. In the first slot, the source transmits the signal $\sqrt{a_1 P_s}\, s_1 + \sqrt{a_2 P_s}\, s_2$ simultaneously to the relay and destination modems, where P_s denotes the source transmit power, s_1 and s_2 are the first and second data symbols normalized as $\mathbb{E}[|s_i|^2] = 1$, where $i \in \{1, 2\}$, and a_1 and a_2 are the power allocation coefficients for the destination and relay modems, respectively. It is assumed that the source-to-destination link has higher attenuation and hence we use $a_1 > a_2$; note that $a_1 + a_2 = 1$. In this regard, the received signals at the relay and destination during the first time slot can be given respectively as

$$y_{\text{r}}^{i} = \left(\sqrt{a_1 P_s}\, s_1 + \sqrt{a_2 P_s}\, s_2\right) A_{\text{sr}}(f, d_{\text{sr}})\, h_{\text{sr}} + n_{\text{r}}, \tag{2}$$

$$y_{\text{d}}^{i} = \left(\sqrt{a_1 P_s}\, s_1 + \sqrt{a_2 P_s}\, s_2\right) A_{\text{sd}}(f, d_{\text{sd}})\, h_{\text{sd}} + n_{\text{d}}, \tag{3}$$

where n_{r} and n_{d} represent the noise at the relay and destination modems with variances σ_{r}^2 and σ_{d}^2, respectively. This noise typically consists of two components: background and impulsive noise [21]–[23].

In the second time slot, assuming that the relaying modem successfully decodes the symbol s_2, the relay will forward this symbol to the destination, using its total power P_r, and therefore the received signal at the destination can be written as

$$y_{\text{d}}^{ii} = \sqrt{P_r}\, A_{\text{rd}}(f, d_{\text{rd}})\, h_{\text{rd}} s_2 + n_{\text{d}}. \tag{4}$$

A. CONVENTIONAL NOMA-PLC

In this approach, both the relay and destination modems use the signals in (2) and (3) to decode the symbol s_1 during the first time slot while treating s_2 as noise. Therefore, using (2) and (3) along with the substitutions $A_i = A_i(f, d_i)$, $\sigma^2 = \sigma_{\text{r}}^2 = \sigma_{\text{d}}^2$, $P = P_{\text{s}} = P_{\text{r}}$ and $\rho = P/\sigma^2$, the signal-to-noise ratio (SNR) associated to the detection of s_1 at the relay and destination can be written respectively as

$$\gamma_{\text{r}}^{i} = \frac{a_1 \rho\, A_{\text{sr}}^2 h_{\text{sr}}^2}{a_2 \rho\, A_{\text{sr}}^2 h_{\text{sr}}^2 + 1} \tag{5}$$

$$\gamma_{\text{d}}^{i} = \frac{a_1 \rho\, A_{\text{sd}}^2 h_{\text{sd}}^2}{a_2 \rho\, A_{\text{sd}}^2 h_{\text{sd}}^2 + 1}. \tag{6}$$

After implementing SIC at the relay, we obtain s_2 and its corresponding SNR is $\gamma_{\text{r}}^{ii} = a_2 \rho\, A_{\text{sr}}^2 h_{\text{sr}}^2$. Note that perfect SIC is assumed here which is a typical assumption done in most of the literature on NOMA, e.g., [24]–[27]. On the other hand, the destination modem decodes s_2 from (4) and its corresponding SNR is $\gamma_{\text{d}}^{ii} = \rho\, A_{\text{rd}}^2 h_{\text{rd}}^2$.

B. IMPROVED NOMA-PLC

Unlike the conventional NOMA-PLC scheme which uses the principle of NOMA only during the first time slot, in the improved NOMA-PLC approach, NOMA is implemented also in the second time slot.[1] In this respect, the relay forwards the two symbols to the destination using the power allocation coefficients a_3 and a_4 as $\sqrt{a_3 P}\, s_1 - \sqrt{a_4 P}\, s_2$, where $a_3 + a_4 = 1$. Therefore, the received signal at the destination modem in the second time slot can be given by

$$y_{\text{d}}^{II} = \left(\sqrt{a_3 P}\, s_1 - \sqrt{a_4 P}\, s_2\right) A_{\text{rd}}\, h_{\text{rd}} + n_{\text{d}}. \tag{7}$$

Now, to obtain interference-free signals at the destination from (3) and (7), linear combination is implemented, i.e., $y_{\text{d}}^{i}\sqrt{a_4}\, h_{\text{rd}} + y_{\text{d}}^{II}\sqrt{a_2}\, h_{\text{sd}}$ and $y_{\text{d}}^{i}\sqrt{a_3}\, h_{\text{rd}} - y_{\text{d}}^{II}\sqrt{a_1}\, h_{\text{sd}}$. Hence, the target signals become

$$T_{\text{I}} = \prod_{i \in \{\text{sd,rd}\}} A_i\, h_i\, \kappa \sqrt{P} s_1 + \sqrt{a_4} A_{\text{rd}}\, h_{\text{rd}}\, n_{\text{d}} + \sqrt{a_2} A_{\text{sd}}\, h_{\text{sd}}\, n_{\text{d}} \tag{8}$$

$$T_{\text{II}} = \prod_{i \in \{\text{sd,rd}\}} A_i\, h_i\, \kappa \sqrt{P} s_2 + \sqrt{a_3} A_{\text{rd}}\, h_{\text{rd}}\, n_{\text{d}} + \sqrt{a_1} A_{\text{sd}}\, h_{\text{sd}}\, n_{\text{d}}, \tag{9}$$

where $\kappa = \sqrt{a_1 a_4} + \sqrt{a_2 a_3}$.

Using (8) and (9), the SNRs of the symbols s_1 and s_2 at the destination can be written respectively as

$$\gamma_{\text{d}}^{\text{I}} = \frac{\prod_{i \in \{\text{sd,rd}\}} A_i^2\, h_i^2 \kappa^2 \rho}{a_4 A_{\text{rd}}^2\, h_{\text{rd}}^2 + a_2 A_{\text{sd}}^2\, h_{\text{sd}}^2} \tag{10}$$

$$\gamma_{\text{d}}^{\text{II}} = \frac{\prod_{i \in \{\text{sd,rd}\}} A_i^2\, h_i^2 \kappa^2 \rho}{a_3 A_{\text{rd}}^2\, h_{\text{rd}}^2 + a_1 A_{\text{sd}}^2\, h_{\text{sd}}^2}. \tag{11}$$

It is worth pointing out that the SNRs at the relay in both the conventional and improved NOMA-PLC systems are equal; however, the SNRs at the destination are different.

C. DECODING STRATEGY

Unlike many communication channels, noise over power lines consists of two main components, namely, background and impulsive noise. The capacity over such channels is determined based on the decoding strategy adopted which can be either erasure (where the samples contaminated by impulsive noise are disregarded), or non-erasure−also referred to as full decoding. The erasure and non-erasure capacities are given respectively as [3]

$$C_{\text{easure}} = (1 - p)\, C_{\text{b}} \tag{12}$$

$$C_{\text{non-easure}} = (1 - p)\, C_{\text{b}} + p\, C_{\text{imp}} \tag{13}$$

where p is the impulsive noise probability, C_{b} and C_{imp} represent the capacity when the channel is contaminated by only Gaussian noise or impulsive noise, respectively. It should be pointed out at this stage that the erasure capacity will be the main focus of our analysis in this paper.

[1] Note that this scheme has been studied in the context of wireless channels in [28].

III. PERFORMANCE ANALYSIS

In this section, we analyze the average capacity of the improved and conventional NOMA-PLC systems and derive accurate analytical expressions for this performance metric.

A. IMPROVED NOMA-PLC SYSTEM

The overall average capacity in this system, $C_{\rm p}$, consists of two rates associated with the first and second symbols, represented respectively by $C_{\rm p1}$ and $C_{\rm p2}$; that is $C_{\rm p} = C_{\rm p1} + C_{\rm p2}$.

Using (12), and because the signal s_1 is also decoded at the relay, the capacity associated with it can be written as

$$C_{\rm p1} = \frac{1-p}{2}\min\left\{\log_2\left(1+\gamma_{\rm r}^{i}\right),\ \log_2\left(1+\gamma_{\rm d}^{\rm I}\right)\right\}, \tag{14}$$

where $\gamma_{\rm r}^{i}$ and $\gamma_{\rm d}^{\rm I}$ are respectively the SNRs at the relay and destination during the first time slot; both of which are defined in the previous section.

On the other hand, the instantaneous capacity associated with the second data symbol can be determined as

$$C_{\rm p2} = \frac{1-p}{2}\min\left\{\log_2\left(1+\gamma_{\rm r}^{ii}\right),\ \log_2\left(1+\gamma_{\rm d}^{\rm II}\right)\right\}. \tag{15}$$

The factor $\frac{1}{2}$ in (14) and (15) is because the end-to-end communication is accomplished over two phases.

To derive the average capacity of the first data symbol, we first rewrite (14) in the following form

$$C_{\rm p1} = \frac{1-p}{2}\log_2\left(1+\min\left\{\gamma_{\rm r}^{i},\ \gamma_{\rm d}^{\rm I}\right\}\right). \tag{16}$$

Now, letting $X = \min\left\{\gamma_{\rm r}^{i}, \gamma_{\rm d}^{\rm I}\right\}$, the average capacity $C_{\rm p1}$ can be calculated as

$$\mathbb{E}\left\{C_{\rm p1}\right\} = \frac{1-p}{2}\int_0^{\infty}\log_2\left(1+z\right) f_X\left(z\right)\,{\rm d}z, \tag{17}$$

where $f_X(\cdot)$ is the PDF of the random variable X.

Another approach to calculate the capacity in (17) is by using the CDF or CCDF of X; that is

$$\begin{aligned}\mathbb{E}\left\{C_{\rm p1}\right\} &= \frac{1-p}{2\ln(2)}\int_0^{\infty}\frac{1-F_X\left(z\right)}{1+z}\,{\rm d}z\\ &= \frac{1-p}{2\ln(2)}\int_0^{\infty}\frac{\bar{F}_X\left(z\right)}{1+z}\,{\rm d}z,\end{aligned} \tag{18}$$

where $F_X(\cdot)$ and $\bar{F}_X(\cdot)$ are respectively the CDF and CCDF of X, which are related as $\bar{F}_X\left(z\right) = 1 - F_X\left(z\right)$.

For simplicity, $\gamma_{\rm r}^{i}$ and $\gamma_{\rm d}^{\rm I}$ are considered to be independent; hence, the CCDF of X can be expressed as

$$\bar{F}_X\left(z\right) = \bar{F}_{\gamma_{\rm r}^{i}}\left(z\right)\bar{F}_{\gamma_{\rm d}^{\rm I}}\left(z\right), \tag{19}$$

where $\bar{F}_{\gamma_{\rm r}^{i}}(\cdot)$ and $\bar{F}_{\gamma_{\rm d}^{\rm I}}(\cdot)$ are the CCDFs of the random variables $\gamma_{\rm r}^{i}$ and $\gamma_{\rm d}^{\rm I}$, respectively.

Using (5), we can express the first CCDF, $\bar{F}_{\gamma_{\rm r}^{i}}\left(z\right)$, as

$$\bar{F}_{\gamma_{\rm r}^{i}}\left(z\right) = \Pr\left\{\frac{a_1\rho\, h_{\rm sr}^2 A_{\rm sr}^2}{a_2\rho\, h_{\rm sr}^2 A_{\rm sr}^2 + 1} > z\right\}, \tag{20}$$

which with some basic mathematical manipulations can be written as

$$\bar{F}_{\gamma_{\rm r}^{i}}\left(z\right) = \Pr\left\{h_{\rm sr}^2 > \frac{z}{\rho\left(a_1 - a_2\, z\right)A_{\rm sr}^2}\right\}. \tag{21}$$

We know that $h_{\rm sr}^2$ is log-normally distributed with parameters $h_{\rm sr}^2 \sim \ln\mathcal{N}\left(2\mu_{\rm sr}, 4\sigma_{\rm sr}^2\right)$. Hence, using the log-normal distribution properties, we can write the CCDF in (21) as follows

$$\bar{F}_{\gamma_{\rm r}^{i}}\left(z\right) = Q\left(\frac{\xi\ln\left(z\right) - 2\mu_{\rm sr} - \xi\ln\left(\left(a_1 - a_2 z\right)\rho A_{\rm sr}^2\right)}{2\sigma_{\rm sr}}\right), \tag{22}$$

where $Q(\cdot)$ denotes the Q-function defined as

$$Q\left(x\right) = \frac{1}{\sqrt{2\pi}}\int_x^{\infty}\exp\left(-\frac{t^2}{2}\right)\,{\rm d}t. \tag{23}$$

On the other hand, using (10), we can write the second CCDF in (19), $\bar{F}_{\gamma_{\rm d}^{\rm I}}\left(z\right)$, as follows

$$\bar{F}_{\gamma_{\rm d}^{\rm I}}\left(z\right) = \Pr\left\{\frac{h_{\rm sd}^2 h_{\rm rd}^2 A_{\rm sd}^2 A_{\rm rd}^2 \rho\varsigma^2}{a_2 h_{\rm sd}^2 A_{\rm sd}^2 + a_4 h_{\rm rd}^2 A_{\rm rd}^2} > z\right\}, \tag{24}$$

which can also be expressed

$$\bar{F}_{\gamma_{\rm d}^{\rm I}}\left(z\right) = \Pr\left\{h_{\rm rd}^2 > \frac{a_2 h_{\rm sd}^2 z}{A_{\rm rd}^2\left(h_{\rm sd}^2 A_{\rm sd}^2\rho\varsigma^2 - a_4 z\right)}\right\}. \tag{25}$$

Depending on whether the denominator in (25) is positive or negative, $\bar{F}_{\gamma_{\rm d}^{\rm I}}\left(z\right)$ can be given by

$$\bar{F}_{\gamma_{\rm d}^{\rm I}}\left(z\right) = \Pr\left(h_{\rm rd}^2 < \frac{a_2 h_{\rm sd}^2 A_{\rm sd}^2 z}{A_{\rm rd}^2\left(h_{\rm sd}^2 A_{\rm sd}^2\rho\varsigma^2 - a_4 z\right)}\,\middle|\, h_{\rm sd}^2 < \varphi\right), \tag{26}$$

where $\varphi = \frac{z a_4}{A_{\rm sd}^2\rho\varsigma^2}$.

We can now mathematically calculate (26) as follows

$$\begin{aligned}\bar{F}_{\gamma_{\rm d}^{\rm I}}\left(z\right) &= 1 - \int_0^{\varphi} f_{h_{\rm sd}^2}\left(u\right)\,{\rm d}u,\\ &\quad + \int_{\varphi}^{\infty} f_{h_{\rm sd}^2}\left(u\right)\underbrace{\Pr\left(h_{\rm rd}^2 \le \frac{a_2 A_{\rm sd}^2 u\, z}{A_{\rm rd}^2\left(\varsigma^2\rho A_{\rm sd}^2 u - a_4 z\right)}\right)}_{F_{h_{\rm rd}^2}\left(u\right)}{\rm d}u\end{aligned} \tag{27}$$

where

$$f_{h_{\rm sd}^2}\left(u\right) = \frac{\xi}{u\sqrt{8\pi\sigma_{h_{\rm sd}}^2}}\exp\left(-\frac{\left(\xi\ln\left(u\right) - 2\mu_{h_{\rm sd}}\right)^2}{8\sigma_{h_{\rm sd}}^2}\right) \tag{28}$$

and

$$F_{h_{\rm rd}^2}\left(u\right) = 1 - Q\left(\frac{\xi\ln\left(a_2 A_{\rm sd}^2 z\, u\right) - 2\mu_{h_{\rm rd}} - \xi\ln\left(\Gamma\right)}{2\sigma_{h_{\rm rd}}}\right), \tag{29}$$

where $\Gamma = A_{\rm rd}^2\left(\varsigma^2\rho\, u A_{\rm sd}^2 - a_4 z\right)$.

Substituting (28) and (29) into (27), along with some basic mathematical manipulations, we get

$$\bar{F}_{\gamma_{\rm d}^{\rm I}}(z) = \frac{\xi}{\sqrt{8\pi\sigma_{h_{\rm sd}}^2}}\int_{\varphi}^{\infty}\frac{1}{u}\exp\left(-\frac{\left(\xi\ln(u)-2\mu_{h_{\rm sd}}\right)^2}{8\sigma_{h_{\rm sd}}^2}\right) \times Q\left(\frac{\xi\ln\left(a_2A_{\rm sd}^2 z\,u\right)-2\mu_{h_{\rm rd}}-\xi\ln(\Gamma)}{2\sigma_{h_{\rm rd}}}\right)\mathrm{d}u. \tag{30}$$

Finally, after substituting $\bar{F}_{\gamma_{\rm r}^{i}}(z)$, (22), and $\bar{F}_{\gamma_{\rm d}^{\rm I}}(z)$, (30), into (19) and then into (18) while modifying the integral's limits, we can calculate the average capacity of the first data symbol as follows

$$\mathbb{E}\left\{C_{\rm p1}\right\} = \frac{1-p}{2\ln(2)}\int_{0}^{\frac{a_1}{a_2}}\frac{\bar{F}_{\gamma_{\rm r}^{i}}(z)\,\bar{F}_{\gamma_{\rm d}^{\rm I}}(z)}{1+z}\,\mathrm{d}z. \tag{31}$$

Following the same procedure above, we can now derive the average capacity associated with the second data symbol, $\mathbb{E}\left\{C_{\rm p2}\right\}$. Let $Y = \min\left\{\gamma_{\rm r}^{ii}, \gamma_{\rm d}^{\rm II}\right\}$, then the CCDF of Y can be expressed as

$$\bar{F}_{Y}(z) = \bar{F}_{\gamma_{\rm r}^{ii}}(z)\;\bar{F}_{\gamma_{\rm d}^{\rm II}}(z) \tag{32}$$

where $\bar{F}_{\gamma_{\rm r}^{ii}}(\cdot)$ and $\bar{F}_{\gamma_{\rm d}^{\rm II}}(\cdot)$ are the CCDFs of $\gamma_{\rm r}^{ii}$ and $\gamma_{\rm d}^{\rm II}$, respectively.

It is straightforward to show that

$$\bar{F}_{\gamma_{\rm r}^{ii}}(z) = Q\left(\frac{\xi\ln(z)-2\mu_{h_{\rm sr}}-\xi\ln\left(\rho\,a_2A_{\rm sr}^2\right)}{2\sigma_{h_{\rm sr}}}\right). \tag{33}$$

Similarly, starting from (11), we can easily show that

$$\bar{F}_{\gamma_{\rm d}^{\rm II}}(z) = \frac{\xi}{\sqrt{8\pi\sigma_{h_{\rm sd}}^2}}\int_{\psi}^{\infty}\frac{1}{u}\exp\left(-\frac{\left(\xi\ln(u)-2\mu_{h_{\rm sd}}\right)^2}{8\sigma_{h_{\rm sd}}^2}\right) \times Q\left(\frac{\xi\ln\left(a_1A_{\rm sd}^2 z\,u\right)-2\mu_{h_{\rm rd}}-\xi\ln(\Delta)}{2\sigma_{h_{\rm rd}}}\right)\mathrm{d}u, \tag{34}$$

where $\psi = \frac{z a_3}{\rho\varsigma^2 A_{\rm sd}^2}$ and $\Delta = A_{\rm rd}^2\left(\varsigma^2\rho\,uA_{\rm sd}^2 - a_3 z\right)$.

After obtaining $\bar{F}_{\gamma_{\rm r}^{ii}}(z)$, (33), and $\bar{F}_{\gamma_{\rm d}^{\rm II}}(z)$, (34), we can now calculate $\mathbb{E}\left\{C_{\rm p2}\right\}$ as

$$\mathbb{E}\left\{C_{\rm p2}\right\} = \frac{1-p}{2\ln(2)}\int_{0}^{\infty}\frac{\bar{F}_{\gamma_{\rm r}^{ii}}(z)\,\bar{F}_{\gamma_{\rm d}^{\rm II}}(z)}{1+z}\,\mathrm{d}z. \tag{35}$$

Finally, the overall average capacity of the improved NOMA-PLC system can be given by

$$\mathbb{E}\left\{C_{\rm p}\right\} = \mathbb{E}\left\{C_{\rm p1}\right\} + \mathbb{E}\left\{C_{\rm p2}\right\}. \tag{36}$$

It is worth noting that optimizing the power allocation coefficients is crucial to maximize the system performance. However, due to the complexity of the capacity expression in (36), it is very challenging to obtain closed-form expressions for the optimal power allocation coefficients. We will therefore conduct in the results section extensive computer simulations to find the optimal values of these parameters that will offer the maximum achievable capacity. This will be obtained as follows

$$\begin{aligned}&\underset{a_i,\,i\in\{1,3\}}{\text{maximize}}\; C_{\rm p}\left(a_i,\,A_m^2,\,\sigma_m^2,\,\mu_m,\,d_m p,\,\rho\right)\\ &\text{subject to } 0 < a_1 < 1\\ &\qquad\qquad 0 < a_3 < 1,\end{aligned} \tag{37}$$

where $m \in \{\text{sr, rd, sd}\}$. This optimization problem will be solved numerically using the exhaustive search method.

In order to clearly highlight the achievable capacity gains using the improved NOMA-PLC approach, we next analyze the performance of the conventional NOMA-PLC system. This is important to make this work self-contained. Note that the approach used here to derive the average capacity for both NOMA-PLC systems is different from that followed in [13].

B. CONVENTIONAL NOMA-PLC SYSTEM

In this system, the principle of NOMA is only implemented at the source modem and the overall capacity, C_c, is also given by the sum of two capacities associated with s_1 ($C_{\rm c1}$) and s_2 ($C_{\rm c1}$); that is $C_{\rm c} = C_{\rm c1} + C_{\rm c2}$.

The capacity associated with s_1 can be expressed as

$$C_{\rm c1} = \frac{1-p}{2}\log_2\left(1+\min\left\{\gamma_{\rm r}^{\rm i},\,\gamma_{\rm d}^{\rm i}\right\}\right), \tag{38}$$

where $\gamma_{\rm r}^{\rm i}$ and $\gamma_{\rm d}^{\rm i}$ are defined in (5) and (6), respectively.

Letting $W = \min\left\{\gamma_{\rm r}^{\rm i},\,\gamma_{\rm d}^{\rm i}\right\}$ and because the random variables $\gamma_{\rm r}^{\rm i}$ and $\gamma_{\rm d}^{\rm i}$ are independent, the CCDF of W can be calculated as $\bar{F}_{W}(z) = \bar{F}_{\gamma_{\rm r}^{\rm i}}(z)\,\bar{F}_{\gamma_{\rm d}^{\rm i}}(z)$, where $\bar{F}_{\gamma_{\rm r}^{\rm i}}(z)$ is the CCDF of $\gamma_{\rm r}^{\rm i}$, given by (22), and $\bar{F}_{\gamma_{\rm d}^{\rm i}}(z)$ is the CCDF of $\gamma_{\rm d}^{\rm i}$ calculated as follows. Using (6), we can express $\bar{F}_{\gamma_{\rm d}^{\rm i}}(z)$ as

$$\bar{F}_{\gamma_{\rm d}^{\rm i}}(z) = \Pr\left\{\frac{a_1\rho\,A_{\rm sd}^2h_{\rm sd}^2}{a_2\rho\,A_{\rm sd}^2h_{\rm sd}^2+1} > z\right\}, \tag{39}$$

which can also be written as

$$\bar{F}_{\gamma_{\rm d}^{\rm i}}(z) = \Pr\left\{h_{\rm sd}^2 > \frac{z}{\rho\,(a_1-a_2\,z)\,A_{\rm sd}^2}\right\}. \tag{40}$$

Because $h_{\rm sd}^2$ is log-normally distributed with parameters $h_{\rm sd}^2 \sim \ln\mathcal{N}\left(2\mu_{\rm sd}, 4\sigma_{\rm sd}^2\right)$, using the properties of log-normal distribution, we can write the CCDF, $\bar{F}_{\gamma_{\rm d}^{\rm i}}(z)$, in the following form

$$\bar{F}_{\gamma_{\rm d}^{\rm i}}(z) = Q\left(\frac{\xi\ln(z)-2\mu_{\rm sd}-\xi\ln\left((a_1-a_2z)\,\rho A_{\rm sd}^2\right)}{2\sigma_{\rm sd}}\right). \tag{41}$$

Substituting (22) and (41) into

$$\mathbb{E}\left\{C_{\rm c1}\right\} = \frac{(1-p)}{2\ln(2)}\int_{0}^{\infty}\frac{\bar{F}_{\gamma_{\rm r}^{\rm i}}(z)\,\bar{F}_{\gamma_{\rm d}^{\rm i}}(z)}{1+z}\,\mathrm{d}z \tag{42}$$

yields the average capacity of the first data symbol given by

$$\mathbb{E}\left\{C_{\rm c1}\right\} = \frac{1-p}{2\ln(2)}\int_{0}^{\frac{a_1}{a_2}}\frac{1}{1+z}\prod_{i\in\{\rm sr,sd\}}$$

$$\times Q\left(\frac{\xi \ln(z) - 2\mu_i - \xi \ln\left((a_1 - a_2 z)\,\rho A_i^2\right)}{2\sigma_i}\right) \mathrm{d}z. \tag{43}$$

Similarly, we now derive the average capacity associated with the second symbol. The capacity of this symbol can be determined using

$$C_{c2} = \frac{1-p}{2}\log_2\left(1 + \min\left\{\gamma_r^{ii},\ \gamma_d^{ii}\right\}\right). \tag{44}$$

Now, let $M = \min\left\{\gamma_r^{ii},\ \gamma_d^{ii}\right\}$, the CCDF of M is $\bar{F}_M(z) = \bar{F}_{\gamma_r^{ii}}(z)\,\bar{F}_{\gamma_d^{ii}}(z)$, where $\bar{F}_{\gamma_r^{ii}}(\cdot)$ is the CCDF of γ_r^{ii}, given by (33), and $\bar{F}_{\gamma_d^{ii}}(\cdot)$ denotes the CCDF of γ_d^{ii} which can be straightforwardly shown to have the following form

$$\bar{F}_{\gamma_d^{ii}}(z) = Q\left(\frac{\xi \ln(z) - 2\mu_{rd} - \xi \ln\left(a_1 \rho A_{rd}^2\right)}{2\sigma_{rd}}\right). \tag{45}$$

Now, substituting the values of $\bar{F}_{\gamma_r^{ii}}(z)$ and $\bar{F}_{\gamma_d^{ii}}(z)$ into

$$\mathbb{E}\{C_{c2}\} = \frac{1-p}{2\ln(2)}\int_0^\infty \frac{\bar{F}_{\gamma_r^{ii}}(z)\,\bar{F}_{\gamma_d^{ii}}(z)}{1+z}\,\mathrm{d}z \tag{46}$$

gives the average capacity associated with the second symbol as

$$\mathbb{E}\{C_{c2}\} = \frac{1-p}{2\ln(2)}\int_0^\infty \frac{1}{1+z}\prod_{\substack{i\in\{sr,rd\}\\ j\in\{1,2\}}} \times Q\left(\frac{\xi \ln(z) - 2\mu_i - \xi \ln\left(a_j P A_i^2\right)}{2\sigma_i}\right)\mathrm{d}z. \tag{47}$$

Finally, using (43) and (47), the overall average capacity of the conventional NOMA-PLC system can be calculated as

$$\mathbb{E}\{C_c\} = \mathbb{E}\{C_{c1}\} + \mathbb{E}\{C_{c2}\}. \tag{48}$$

The maximum achievable average capacity for this system that corresponds to the optimal values of the power allocation coefficients can be determined using

$$\begin{aligned} &\underset{a_1}{\text{maximize}}\ C_c\left(a_1,\ A_m^2,\ \sigma_m^2,\ \mu_m,\ d_m p,\ \rho\right)\\ &\text{subject to } 0 < a_1 < 1 \end{aligned} \tag{49}$$

Similar to the previous section, this optimization problem will be solved numerically using the exhaustive search method.

IV. RESULTS AND DISCUSSIONS

In this section, we present and discuss some numerical examples obtained using the derived analytical expressions above. Monte Carlo simulations are included and are averaged over 10^6 channel realizations. The impact of several system parameters on the performance of both improved and conventional NOMA-PLC systems are investigated. Throughout this section, we adopt a common cable attenuation model given by

$$A_i(f, d_m) = e^{-(b_o + b_1 f^k) d_m}, \tag{50}$$

where $m \in \{sr, rd, sd\}$, f is the operating frequency in MHz, k is the exponent of the attenuation factor, b_o and b_1 are constants obtained from measurements. All the results below are based on the following parameters: $b_0 = 9.4 \times 10^{-3}$, $b_1 = 4.2 \times 10^{-7}$, $k = 0.7, f = 30$MHz [1]. It is worth noting that the same parameters were used in previous analysis, see e.g., [12], [29], [30].

To begin with, we plot in Fig. 2 the analytical and simulated average capacities with respect to the transmit SNR for both the improved and conventional NOMA-PLC systems with various values of the channel variance and end-to-end distance.[2] In these results, the relay is placed $\frac{d_{sd}}{3}$m away from the source modem. Clearly, the good match between the analytical results and the simulations indicates the accuracy of our analysis. It is also clear that the improved NOMA-PLC approach always outperforms the conventional scheme for all the given system configurations. Evidently, as the transmit SNR increases, the average sum capacity performance enhances and more so when the channel variances are relatively small. The other observation one can see from these results is that when the source and destination modems become more distant, the performance deteriorates considerably. It is interesting to highlight the fact that for a given average capacity requirement, the transmit SNR will be considerably lower for the improved NOMA-PLC system relative to that of the conventional NOMA-PLC system. As an example, consider the scenario in Fig. 2a when the end-to-end distance is 100m and the capacity requirement is 3 bits/sec/Hz. With this in mind, having a closer look at this figure, it is clear that a such requirement can be met by the improved system with 10dB less in the transmit power compared to the conventional system. This is of utmost importance because it allows reducing electromagnetic emissions from the power lines.

Furthermore, the power allocation coefficients and the impulsive noise probability are crucial parameters in determining the performance of the systems under consideration. Therefore, we now investigate the influence of these parameters on the average capacity of both the improved and conventional NOMA-PLC systems. Fig. 3 depicts the average capacity as a function of the power allocation coefficient a_1 with several values of the impulsive noise probability. Note that in this evaluation, the relay is positioned midway between the end modems. It is apparent that for the same given average capacity and noise probability, the improved NOMA-PLC system has better performance than that of the conventional one. In addition, increasing the noise probability will always deteriorate the performance. Another important observation is that when a_1 is either too small or too large, the performance will be very poor. Therefore, there exists an optimal value for the power allocation coefficient that maximizes performance. This is true for all the systems and noise probabilities considered. A clear difference between the

[2]Note that increasing the number of network branches translates into an increase in the channel variance.

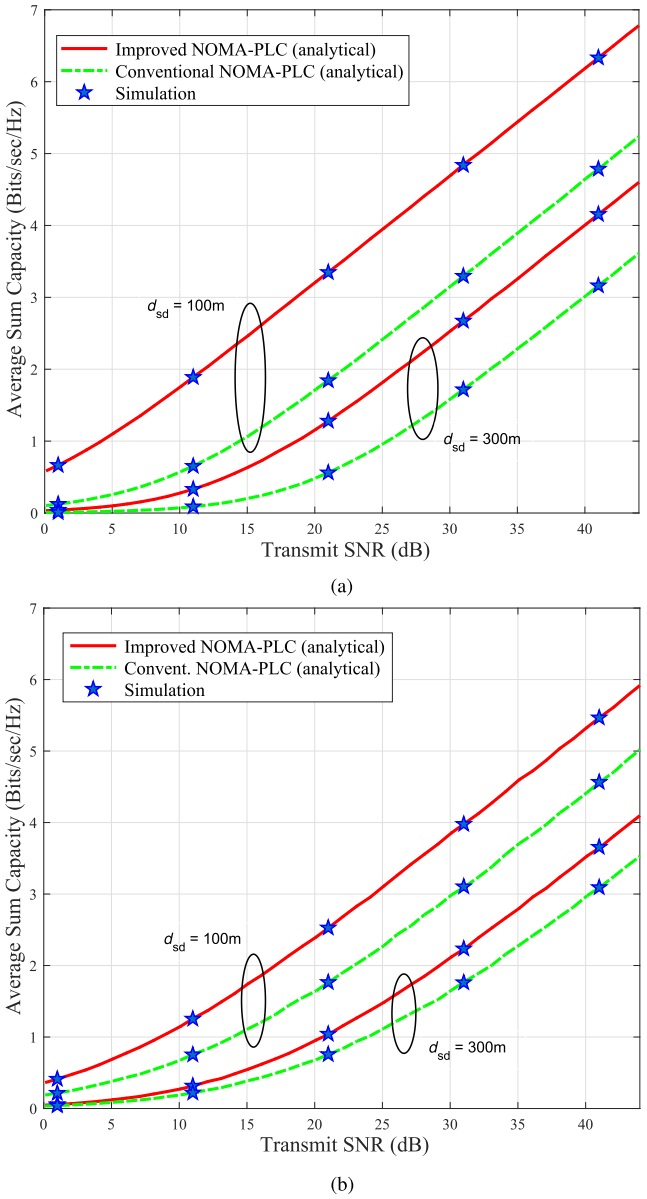

FIGURE 2. Average capacity performance as a function of the transmit SNR with different channel variances and end-to-end distances for both the improved and conventional NOMA-PLC systems. In these results, it is assumed that $d_{sr} = d_{sd}/3$. (a) $\sigma_{sr} = \sigma_{rd} = \sigma_{sd} = 1$dB. (b) $\sigma_{sr} = \sigma_{rd} = \sigma_{sd} = 5$dB.

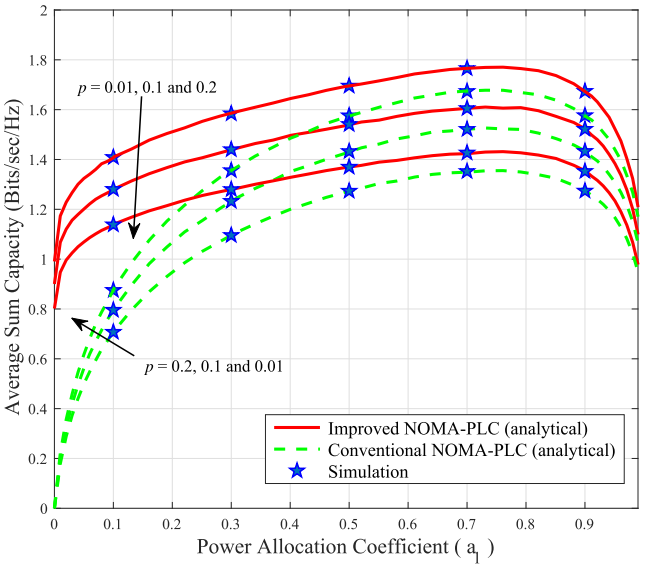

FIGURE 3. Average capacity as a function of a_1 with various impulsive noise probabilities for both the improved and conventional NOMA-PLC systems. Note that the relay is placed midway between the end modems, $d_3 = 200$ m, SNR = 15dB, $a_3 = 0.7$ and $\sigma_{sr} = \sigma_{rd} = \sigma_{sd} = 3$dB.

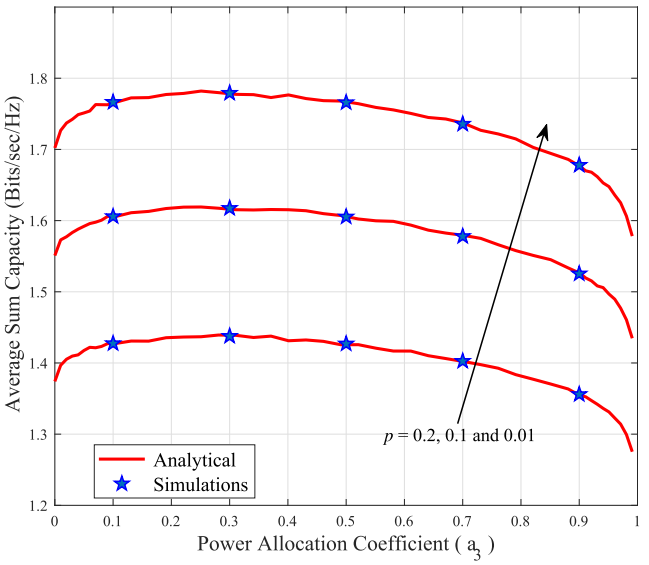

FIGURE 4. Average capacity with respect to a_3 with various impulsive noise probabilities. The relay is placed midway between the end modems $d_3 = 200$m, SNR = 15dB, $a_1 = 0.9$ and $\sigma_{sr} = \sigma_{rd} = \sigma_{sd} = 2$dB.

performance of the improved and conventional techniques is that when a_1 is extremely low, the capacity of the latter system will be close to zero unlike that of the proposed approach. Fig. 4 shows the capacity performance of the improved system with respect to a_3 for several noise probabilities; similar observations can be noticed as in the previous case.

We next plot the maximum achievable average capacities that correspond to the optimal power allocation coefficients for both the enhanced and conventional NOMA-PLC systems. In this regard, extensive search algorithm was used to find the optimal values of a_1 and a_3 using (37) and (49).

The maximum achievable performance is presented in Fig. 5 for different SNR scenarios. It is seen that the optimized enhanced NOMA-PLC system always outperforms the optimized conventional NOMA-PLC scheme for all the system configurations considered. It is also evident that when the end-to-end distance is either too small or too large, the two systems perform similarly. Another result worth highlighting is that the highest performance gain is observed when the distance is intermediate. Last but not least, as anticipated, increasing SNR leads to increasing the capacity in both NOMA-PLC systems.

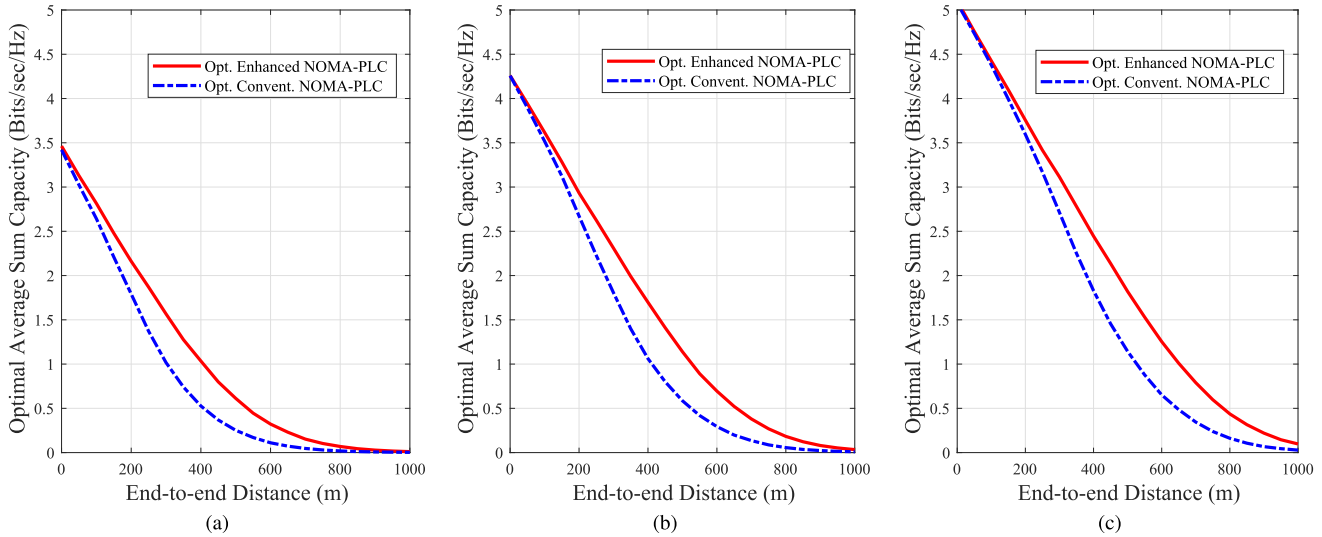

FIGURE 5. Maximum achievable average capacity versus the end-to-end distance for the optimized NOMA-PLC systems. The relay is placed midway between the end modems, $\sigma_{sr} = \sigma_{rd} = \sigma_{sd} = 3$dB and $\mu_{sr} = \mu_{rd} = \mu_{sd} = 3$dB. (a) SNR = 15dB. (b) SNR = 20dB. (c) SNR = 25dB.

V. CONCLUSION

This paper analyzed the performance of NOMA-PLC systems and showed that implementing power allocation to different symbols at both the source and relay modems can considerably increase the average capacity of conventional NOMA-PLC networks. The average capacity was adopted as the main performance metric for which we derived accurate analytical expressions, for both the conventional and improved NOMA-PLC systems. To validate the accuracy of our analysis, computer simulations were provided. The derived expressions allowed us to make meaningful and insightful comparisons between different systems as well as to investigate the impact of various system parameters on the performance. In addition, the optimization problem of the power allocation coefficients was addressed for both NOMA-PLC systems. Results clearly showed that the improved NOMA-PLC system is superior over the conventional one and that the former is able to attain the same performance with less electromagnetic emissions to the surroundings. Increasing the impulsive noise probability and/or the channel variance, which is related to the number of network branches, can significantly impact the average capacity. Finally, it was demonstrated that to maximize the average capacity, the power allocation coefficients must be carefully selected.

REFERENCES

[1] M. Zimmermann and K. Dostert, "A multipath model for the powerline channel," *IEEE Trans. Commun.*, vol. 50, no. 4, pp. 553–559, Apr. 2002.

[2] M. Rozman, A. Ikpehai, B. Adebisi, and K. M. Rabie, "Channel characterisation of cooperative relaying power line communication systems," in *Proc. IEEE Int. Symp. Commun. Syst., Netw. Digit. Signal Process. (CSNDSP)*, Jul. 2016, pp. 1–5.

[3] L. D. Bert, P. Caldera, D. Schwingshackl, and A. M. Tonello, "On noise modeling for power line communications," in *Proc. IEEE Int. Symp. Power Line Commun. Appl. (ISPLC)*, Apr. 2011, pp. 283–288.

[4] *HomePlug AV White Paper*. HomePlug Powerline Alliance, 2005.

[5] *HomePlug AV2 Technology*. HomePlug Powerline Alliance, 2012.

[6] K. B. Carbonaro and G. A. Carrijo, "Performance analysis of m-qam/ofdm systems for PLC under Gaussiano and impulsive noise," *IEEE Latin Amer. Trans.*, vol. 14, no. 1, pp. 109–114, Jan. 2016.

[7] M. Ghosh, "Analysis of the effect of impulse noise on multicarrier and single carrier QAM systems," *IEEE Trans. Commun.*, vol. 44, no. 2, pp. 145–147, Feb. 1996.

[8] G. Ren, S. Qiao, H. Zhao, C. Li, and Y. Hei, "Mitigation of periodic impulsive noise in OFDM-based power-line communications," *IEEE Trans. Power Del.*, vol. 28, no. 2, pp. 825–834, Apr. 2013.

[9] L. Lampe and A. Vinck, "Cooperative multihop power line communications," in *Proc. IEEE Int. Symp. Power Line Commun. Appl. (ISPLC)*, Mar. 2012, pp. 1–6.

[10] K. M. Rabie and B. Adebisi, "Enhanced amplify-and-forward relaying in non-Gaussian PLC networks," *IEEE Access*, vol. 5, pp. 4087–4094, 2017.

[11] A. Dubey and R. K. Mallik, "PLC system performance with AF relaying," *IEEE Trans. Commun.*, vol. 63, no. 6, pp. 2337–2345, Jun. 2015.

[12] K. M. Rabie, B. Adebisi, and H. Gacanin, "Outage probability and energy efficiency of DF relaying power line communication networks: Cooperative and Non-cooperative," in *Proc. IEEE Int. Conf. Commun. (ICC)*, May 2017, pp. 1–6.

[13] K. M. Rabie, B. Adebisi, E. H. Yousif, H. Gacanin, and A. M. Tonello, "A comparison between orthogonal and non-orthogonal multiple access in cooperative relaying power line communication systems," *IEEE Access*, vol. 5, pp. 10118–10129, 2017.

[14] M. S. P. Facina, H. A. Latchman, H. V. Poor, and M. V. Ribeiro, "Cooperative in-home power line communication: Analyses based on a measurement campaign," *IEEE Trans. Commun.*, vol. 64, no. 2, pp. 778–789, Feb. 2016.

[15] A. M. Tonello, F. Versolatto, and A. Pittolo, "In-home power line communication channel: Statistical characterization," *IEEE Trans. Commun.*, vol. 62, no. 6, pp. 2096–2106, Jun. 2014.

[16] A. M. Tonello, F. Versolatto, B. Bejar, and S. Zazo, "A fitting algorithm for random modeling the PLC channel," *IEEE Trans. Power Del.*, vol. 27, no. 3, pp. 1477–1484, Jul. 2012.

[17] K. M. Rabie, B. Adebisi, and A. Salem, "Improving energy efficiency in dual-hop cooperative PLC relaying systems," in *Proc. IEEE Int. Symp. Power Line Commun. Appl. (ISPLC)*, Mar. 2016, pp. 196–200.

[18] K. Khalil, M. G. Gazalet, P. Corlay, F. X. Coudoux, and M. Gharbi, "An MIMO random channel generator for indoor power-line communication," *IEEE Trans. Power Del.*, vol. 29, no. 4, pp. 1561–1568, Aug. 2014.

[19] J. Song, W. Ding, F. Yang, H. Yang, B. Yu, and H. Zhang, "An indoor broadband broadcasting system based on PLC and VLC," *IEEE Trans. Broadcast.*, vol. 61, no. 2, pp. 299–308, Jun. 2015.

[20] H. Gassara, F. Rouissi, and A. Ghazel, "Statistical characterization of the indoor low-voltage narrowband power line communication channel," *IEEE Trans. Electromagn. Compat.*, vol. 56, no. 1, pp. 123–131, Feb. 2014.

[21] M. Zimmermann and K. Dostert, "Analysis and modeling of impulsive noise in broad-band powerline communications," *IEEE Trans. Electromagn. Compat.*, vol. 44, no. 1, pp. 249–258, Feb. 2002.
[22] M. Antoniali, F. Versolatto, and A. M. Tonello, "An experimental characterization of the PLC noise at the source," *IEEE Trans. Power Del.*, vol. 31, no. 3, pp. 1068–1075, Jun. 2016.
[23] S. D'Alessandro, M. D. Piante, and A. M. Tonello, "On modeling the sporadic impulsive noise rate within in-home power line networks," in *Proc. IEEE Int. Symp. Power Line Commun. (ISPLC)*, Mar. 2015, pp. 154–159.
[24] Z. Ding, Z. Yang, P. Fan, and H. V. Poor, "On the performance of non-orthogonal multiple access in 5G systems with randomly deployed users," *IEEE Signal Process. Lett.*, vol. 21, no. 12, pp. 1501–1505, Dec. 2014.
[25] J.-B. Kim and I.-H. Lee, "Capacity analysis of cooperative relaying systems using non-orthogonal multiple access," *IEEE Commun. Lett.*, vol. 19, no. 11, pp. 1949–1952, Nov. 2015.
[26] Y. Zhang, H.-M. Wang, Q. Yang, and Z. Ding, "Secrecy sum rate maximization in non-orthogonal multiple access," *IEEE Commun. Lett.*, vol. 20, no. 5, pp. 930–933, May 2016.
[27] Z. Yang, W. Xu, and Y. Li, "Fair non-orthogonal multiple access for visible light communication downlinks," *IEEE Wireless Commun. Lett.*, vol. 6, no. 1, pp. 66–69, Feb. 2017.
[28] W. Duan, M. Wen, Z. Xiong, and M. H. Lee, "Two-stage power allocation for dual-hop relaying systems with non-orthogonal multiple access," *IEEE Access*, vol. 5, pp. 2254–2261, 2017.
[29] K. M. Rabie, B. Adebisi, A. M. Tonello, and G. Nauryzbayev, "For more energy-efficient dual-hop DF relaying power-line communication systems," *IEEE Syst. J.*, to be published, doi: 10.1109/JSYST.2016.2639321.
[30] K. M. Rabie, B. Adebisi, H. Gacanin, and S. Yarkan, "Energy-per-bit performance of relay-assisted power line communication systems," *IEEE Trans. Green Commun. Netw.*, to be published, doi: 10.1109/TGCN.2018.2794613.

KHALED M. RABIE (S'12–M'15) received the B.Sc. degree (Hons.) in electrical and electronic engineering from the University of Tripoli, Libya, in 2008, and the M.Sc. and Ph.D. degrees in communication engineering from the University of Manchester, U.K., in 2010 and 2015, respectively. He is currently a Research Associate with Manchester Metropolitan University, Manchester, U.K. His research interests include signal processing and analysis of power-line and wireless communication networks. He is a Fellow of the U.K. Higher Education Academy. He was a recipient of several awards including the Agilent Technologies' best M.Sc. Student Award, the Manchester Doctoral College Ph.D. scholarship, and the MMU Outstanding Knowledge Exchange Project award of 2016. He was also a recipient of the best student paper award at the IEEE International Symposium on Power Line Communications and its applications in 2015, Texas, USA. He is the Publication Chair of the 2018 IEEE ISPLC, the IEEE CSNDSP Co-Chair of the Green Communications and Networks Track and an Editor of the Elsevier *Physical Communication Journal*.

BAMIDELE ADEBISI (M'06–SM'15) received the bachelor's degree in electrical engineering from Ahmadu Bello University, Zaria, Nigeria, in 1999, and the master's degree in advanced mobile communication engineering and the Ph.D. degree in communication systems from Lancaster University, U.K., in 2003 and 2009, respectively. He was a Senior Research Associate with the School of Computing and Communication, Lancaster University, from 2005 to 2012. He joined Manchester Metropolitan University, Manchester, in 2012, where he is currently a Reader in electrical and electronic engineering. He has involved in several commercial and government projects focusing on various aspects of wireline and wireless communications. He is particularly interested in research and development of communication technologies for electrical energy monitoring/management, transport, water, critical infrastructures protection, home automation, IoTs, and cyber physical systems. He has several publications and a patent in the research area of data communications over power line networks and smart grid. He is a member of IET.

ANDREA M. TONELLO (M'00–SM'12) received the Dr.Ing. degree (Hons.) in electronics and the D.Res. degree in electronics and telecommunications from the University of Padova, Padova, Italy, in 1996 and 2003, respectively. From 1997 to 2002, he was with the Bell Labs-Lucent Technologies, Whippany, NJ, USA, first as a Member of the Technical Staff. Then, he was promoted to a Technical Manager and appointed as the Managing Director of the Bell Labs Italy Division. In 2003, he joined the University of Udine, Udine, Italy, where he became an Aggregate Professor in 2005 and an Associate Professor in 2014. He is currently the Chair of the Embedded Communication Systems Group, University of Klagenfurt, Klagenfurt, Austria. He is also the Founder of the spin-off company WiTiKee. He was a recipient of the several awards, including the Distinguished Visiting Fellowship from the Royal Academy of Engineering, U.K., in 2010, and the IEEE VTS Distinguished Lecturer Award from 2011 to 2015. He is the Chair of the IEEE Communications Society Technical Committee on Power Line Communications and an Associate editor of the IEEE TRANSACTIONS ON COMMUNICATIONS.

SERHAN YARKAN received the B.S. and M.Sc. degrees in computer science from Istanbul University, Istanbul, Turkey, in 2001 and 2003, respectively, and the Ph.D. degree from the University of South Florida, Tampa, FL, USA, in 2009. He was a Post-Doctoral Research Associate with the Department of Computer and Electrical Engineering, Texas A&M University, College Station, TX, USA, from 2010 to 2012. He is currently an Associate Professor with the Department of Electrical-Electronics Engineering, Istanbul Commerce University, Istanbul. His current research interests include statistical signal processing, cognitive radio, wireless propagation channel measurement and modeling, cross-layer adaptation and optimization, and interference management in next-generation wireless networks and underground mine channels and disaster communications.

MUHAMMAD IJAZ (S'11–M'15) received the M.Sc. degree in optoelectronic and communication engineering with commendation and the Ph.D. degree in free-space optical communications from Northumbria University, Newcastle upon Tyne, U.K., in 2009 and 2013, respectively. After the successful completion of his M.Sc., he received Northumbria University Studentship to pursue his Ph.D. He was a Research Fellow in visible light communication with the University of Edinburgh, U.K., from 2013 to 2015. He worked in modeling and designing a large scale multiple-input multiple-output based visible light communication system using spatial modulation and for novel methods of energy harvesting ideas in the field of wireless communications. He is currently a Lecturer with Manchester Metropolitan University, U.K., in 2015. His specialized areas of research and interests are optical wireless/fibre communications, advanced modulation schemes including OFDM, visible light communication, applications of LiFi, powerline communications, IoTs and photonics, and optical sensors design. He is a member of IET.